160-Gb/s polarization-multiplexing optical NRZ-DQPSK transmission using differential detection

He Wen (闻 和)*, Jinxin Liao (廖金鑫), Xiaoping Zheng (郑小平), and Hanyi Zhang (张汉一)

State Key Laboratory on Integrated Optoelectronics/Tsinghua National Laboratory for Information Science and Technology, Department of Electronic Engineering, Tsinghua University, Beijing 100084, China

**Corresponding author: wen-he@tsinghua.edu.cn*

Received December 23, 2010; accepted May 9, 2011; posted online July 29, 2011

Using differential detection, we perform polarization-multiplexing 160-Gb/s optical non-return-to-zero (NRZ) differential quadrature phase shift keying (DQPSK) signal transmission over 100-km standard single mode fiber at a bit error rate (BER) of less than 10^{-9}. The enabling technology includes clock recovery, fine dispersion compensation, and polarization tracking for de-multiplexing. Furthermore, a hybrid clock recovery scheme is proposed. The scheme is realized with ordinary devices using an optoelectrical modulator to down-convert the clock frequency and a phase-locked loop for filtering, which can provide an indication signal that simultaneously monitors residual dispersion and tracking polarization.

OCIS codes: 060.0060, 230.0230, 060.2230.

doi: 10.3788/COL201109.100607.

Given the ever increasing bandwidth demands (e.g., for imaging, demand of video, gaming, etc.), the capacity of optical transmission systems is being constantly raised through the application of several approaches that include the use of advanced modulation formats with higher spectral efficiency, increasing the symbol rate of each channel, and orthogonal polarization multiplexing with identical wavelengths; these approaches are enabled by coherent detection[1−3]. However, limited by the speed of analog-to-digital converter (ADC) and digital signal processing (DSP) processors, most coherent detection systems have a symbol rate below 30 Gsymbol/s and process data offline[4]. Conversely, differential detection of phase shift keying (PSK) systems can be operated at a higher symbol rate but with relatively simple electronic devices; however, these advantages are achieved at the cost of degraded performance[5]. Enhanced by proper polarization tracking[6,7], this type of system can also support polarization multiplexing through the addition of a polarization beam combiner (PBC) and a polarization beam splitter (PBS) at each end of a fiber link. Moreover, a real-time bit error rate (BER) test can be performed to intuitively evaluate and optimize the system. In this letter, we present a 160-Gb/s polarization-multiplexing (PolM) none-return-to-zero (NRZ) differential quadrature phase-shifted keying (DQPSK) transmission system over 100-km standard single mode fiber (SSMF) enabled by a novel opto-electrical clock recovery (CR) scheme[8], fine dispersion compensation, polarization tracking-based polarization de-multiplexing, and differential detection.

The setup for the PolM NRZ-DQPSK transmission system is shown in Fig. 1. A dual-parallel Mach-Zehnder modulator (DP-MZM) is used to generate the optical NRZ-DQPSK driven by a pair of de-correlated 40-Gb/s NRZ signal output from the data and inverse data ports of an electrical multiplexer (Centellax). The four multiplexed tributaries of the 10-Gb/s NRZ signal come from a pulse pattern generator output by power division and time delay. After the use of the DP-MZM, the signal is separated into two copies with a 2-dB power difference and one signal path is de-correlated with a 30-ns time delay. Subsequently, the two tributaries are combined by a PBC, which results in two independent datasets carried on a pair of orthogonal polarizations. The PolM NRZ-DQPSK is then transmitted over 100-km SSMF with a loss of 19.5 dB and a launch power of 1 dBm. At the receiving end, the signal is power amplified, dispersion compensated, tapped for monitoring and CR, as well as filtered for de-multiplexing, demodulation, and BER measurement. The dispersion compensation unit is composed of a spool of dispersion compensating fiber (DCF)-compensating 80-km SSMF dispersion and a tunable dispersion compensation module (TDCM) with a tuning range of –400 – 400 ps/nm and a tuning step of 10 ps/nm. A variable optical attenuator (VOA) employed before the DCF is applied to keep the input power below –3 dBm. The total link attenuation is 41 dB, including transmission fiber at 19.5 dB, TDCM at 3.5 dB, DCF at 8 dB, attenuator at 9 dB, and optical filter loss at 1 dB. The optical signal-to-noise ratio (OSNR) at the receiver is about 30 dB at 0.1 nm. Limited by the experimental conditions, we do not implement polarization scrambling and tracking. The polarization de-multiplexing is manually implemented by adjusting a polarization controller located before a PBS on the basis of the monitoring signal from the CR unit, instead of directly using the

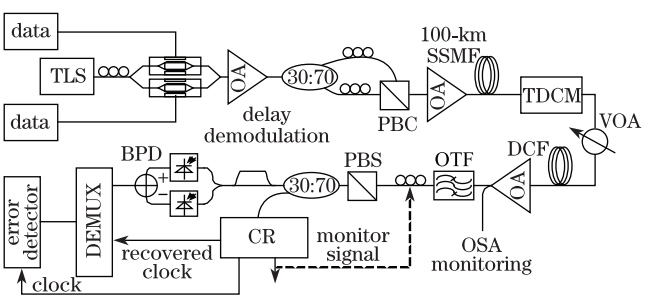

Fig. 1. PolM NRZ-DQPSK transmission system setup. TLS: tunable laser source; OA: optical amplifier; DEMUX: demultiplexer: OTF: optical tunable filter; OSA: optical spectrum analyzer; BPD: balanced photodiode.

signal eye diagram. The de-multiplexed signal is then demodulated with a homemade delay interferometer (DI) composed of a pair of sliced 3-dB couplers; the demodulated I (in-phase) or Q (quadrature) tributary is further de-multiplexed into four tributaries for the BER test, in which a half symbol-rate clock coming from the CR unit is used.

One of the key techniques in this system is CR, which is confronted with challenges such as high operational frequency, as well as expensive devices and modules with moderate performance. For example, extracting a clock by filtering at an amplitude ripple of less than 10% of peak-to-peak amplitude caused by the data pattern effect necessitates a 40-GHz band pass filter with a bandwidth as narrow as 200 MHz. Such a filter is difficult to realize. To address these difficulties, we propose an optoelectrical CR scheme, in which optical domain frequency down-conversion is applied using a MZM; the NRZ-DQPSK passes through the MZM driven by a voltage control oscillator (VCO) harmonic. The frequency down-converted clock is filtered by employing an intermediate-frequency phase locked loop (PLL) with ordinary devices. The principle is described as

$$\begin{aligned} P_{\rm out}(t) &= P_{\rm in}(t)[1-\cos(m\pi\sin\omega t+\phi)]/2 \\ &= P_{\rm in}(t)\Big[\frac{1-{\rm J}_0(m\pi)\cos\phi}{2}-\cos\phi\sum_{n=1}^{\infty}{\rm J}_{2n}(m\pi)\cos(2n\omega t) \\ &\quad +\sin\phi\sum_{n=0}^{\infty}{\rm J}_{2n+1}(m\pi)\sin(2n+1)\omega t\Big], \end{aligned} \tag{1}$$

where $P_{\rm in}$ and $P_{\rm out}$ are the optical powers of the signal input to and output from the MZM, respectively; m is the ratio of the modulation signal amplitude to the MZM half-wave voltage; ϕ denotes the phase shift determined by the MZM bias.

Equation (1) indicates that the output from the MZM contains the mixed products of the input signals and harmonics of the driving signal. By properly filtering and setting the MZM bias, we can obtain the required components.

The proposed CR scheme is depicted in Fig. 2, in which a VCO working at 5 GHz is employed to recover a 20-GHz half-symbol-rate clock by frequency quadrupling; the third harmonic is used to drive the MZM biased at the minimal transmittance. The resultant

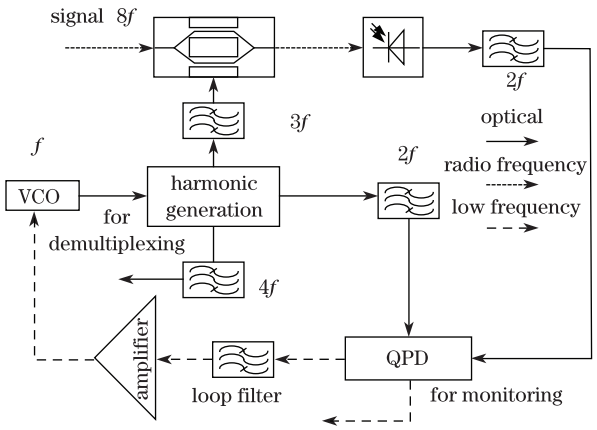

Fig. 2. CR scheme based on optical down-conversion. f represents the frequency.

10-GHz (40-2×3×5) differential frequency signal is photon detected, amplified, and phase locked to the VCO second harmonic by the PLL. All the devices in the CR unit work at speeds less than half of the symbol rate. The frequency of the MZM driving signal is 3/8 of the symbol rate. If the available highest frequency is 40 GHz, the symbol rate can be scaled to 107 Gsymbol/s.

In addition, we place a quadrature phase detector (QPD) in the PLL to simultaneously provide phase error and clock intensity indication signals. The output from the two ports of a QPD is orthogonal. When the PLL is locked, the phase error approaches zero, whereas the other is a direct current (DC) proportional to the multiplication of the VCO and clock amplitudes. Given a constant VCO power, this output uniquely determines the amplitude of the signal clock. Using this signal, we can perform polarization de-multiplexing by maximizing the indicating signal because the power levels of the signals on two polarizations differ[9].

Figure 3 shows the power spectra of the photon-detected signal after passing through the MZM with (dotted) and without (solid) the application of a driving signal of 15-GHz single tone. When the driving signal is applied, the mixed products at 10 GHz and the second-order harmonic at 30 GHz appear. However, the intensity and carrier-to-noise ratio (CNR) of the target product at 10 GHz are lower than those of the 40-GHz clock in the original signal. These results are attributed to the mixing efficiency being lower than the unity and overlap of the mixed products with the original signal spectrum, as predicted by Eq. (1). A tradeoff between reducing the original signal power spectrum interference and increasing the mixing efficiency by optimizing modulation depth m should be considered. This indicates that radio frequency conversion in the optical domain can be realized with low-speed devices but at the cost of a reduced CNR.

In the transmission experiment, the fiber link dispersion is almost completely compensated for by the DCF and TDCM. At this point, the indication signal proportional to the amplitude of the recovered clock reaches a local minimum. By tuning the TDCM to vary the residual dispersion, this signal slightly increases and then drops sharply when the residual dispersion deviates from zero (Fig. 4). This can be explained by the eye diagrams in the inset, which shows that for a low non-zero dispersion, the weak inter-symbol interference (ISI) causes the peak power of some pulses to rise, but for a large dispersion, the ISI spreads over several neighboring symbols, causing the $\pm\pi/2$ phase-shifted pulses to move in opposite directions in the temporal axis. Thus, timing information is destroyed. The result shows that the amplitude of the recovered clock can be used to monitor the residual dispersion of the transmitted signal. The measured BERs increase to a level higher than 10^{-9} at a high OSNR if the residual dispersion increases to more than ± 60 ps/nm, at which point the corresponding clock power is smaller than that at zero dispersion. Consequently, we can use the clock power value at zero dispersion as a low threshold to evaluate whether the residual dispersion is acceptable.

Using the recovered clock and its indication signal amplitude, we can perform fine dispersion compensation,

polarization de-multiplexing, time de-multiplexing, and BER testing. Figure 5 shows the eye diagrams and optical spectra of the generated 80-Gb/s NRZ-DQPSK before DI demodulation, as well as the I and Q tributaries after demodulation at the transmitter. Figure 6 shows the comparison of the eye diagrams of the received signals on two polarizations after transmission and single polarization before transmission. With fine dispersion compensation, no apparent distortion is found. The eye diagrams of the demodulated signal captured by oscilloscope are single-ended detection whereas the ones used for BER test is balanced detection. Because of the weaker power, the eye diagrams of x-polarization are more severely

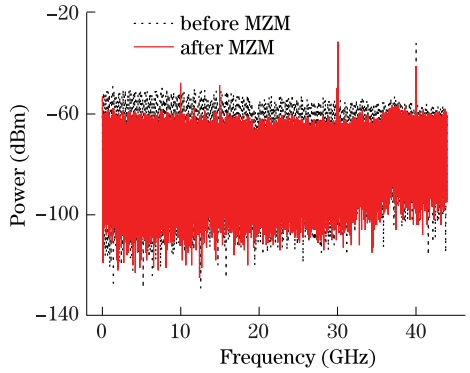

Fig. 3. Power spectra of NRZ-DQPSK intensity after passing through the MZM with (dotted) and without (solid) the application of a driving signal.

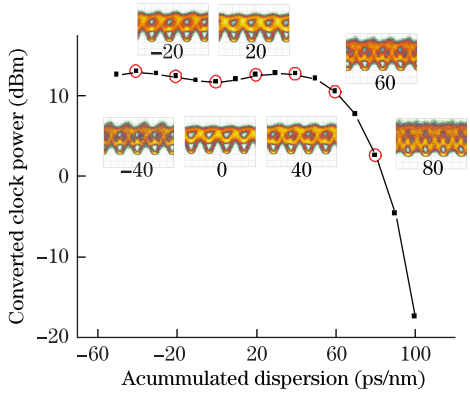

Fig. 4. Extracted clock power versus signal residual dispersion. Insets: eye diagram at the corresponding dispersion marked with a circle.

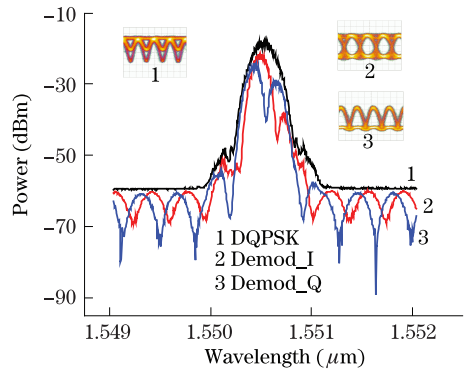

Fig. 5. Eye diagrams and optical spectra of 80-Gb/s NRZ-DQPSK before and after demodulation. Demod: demodulation.

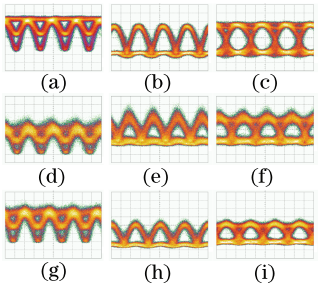

Fig. 6. Eye diagrams of NRZ-DQPSK before and after demodulation. (a)–(c) single polarization, (d)–(f) x-polarization, and (g)–(i) y-polarization. The left columm: NRZ-DQPSK before demodulation; the middle column: destructive port output of DI; the right column: constructive port output of DI.

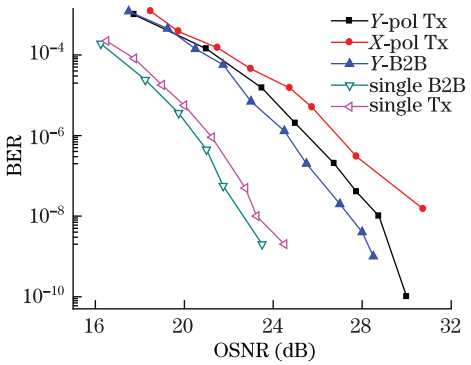

Fig. 7. BER versus OSNR for single polarization and PolM system. pol: polarization; Tx: transmitted; B2B: back-to-back.

degraded by the amplified spontaneous emission noise and intrinsic thermal noise in the oscilloscope. By increasing the signal power, however, error-free receiving can be realized. Figure 7 shows BER versus OSNR for both single polarization and the PolM system before and after transmission. The transmission penalty at BER=10^{-9} is about 1 dB for both systems. However, the required OSNR for the PolM system is 4 dB larger than that required for single polarization, in which 3 dB accounts for the reduced power of each polarization channel, and an extra 1 dB is attributed to the non-ideal isolation of PBS-induced inference in de-multiplexing. The receiving sensitivity at the input of DI is about 5 dBm; such a high level is required so that the balanced detector can generate a signal with its amplitude larger than 100 mV to satisfy the demand of the de-multiplexer.

In conclusion, a PolM 160-Gb/s optical NRZ-QPSK signal transmission over 100-km SSMF by differential detection is performed, enabled by a proposed opto-electrical CR scheme using ordinary devices, fine dispersion compensation, and polarization tracking for de-multiplexing. A BER of less than 10^{-9} is achieved. This system serves as reference for transmissions of 100 Gb/s or higher.

This work was supported in part by the National Natural Science Foundation of China (Nos. 60736003, 61025004, and 61032005) and the National "863" Program of China (Nos. 2009AA01Z223 and 2009AA01Z253).

References

1. X. Zhou, J.-J. Yu, M.-F. Huang, Y. Shao, T. Wang, P. Magill, M. Cvijetic, L. Nelson, M. Birk, G.-D. Zhang, S. Ten, H. B. Matthew, and S. K. Mishra, in *Proceedings of OFC/NFOEC 2009* PDPB4 (2009).
2. H. Gnauck, P. J. Winzer, C. R. Doerr, and L. L. Buhl, in *Proceedings of OFC/NFOEC 2009* PDPB8 (2009).
3. Y. Feng, H. Wen, H. Zhang, and X. Zheng, Chin. Opt. Lett. **8,** 976 (2010).
4. R. Ludwig, J. K. Fischer, A. Matiss, L. Molle, C. C. Le**on**hardt, H.-G. Bach, R. Kunkel, A. Umbach, and C. Schubert, in *Proceedings of ECOC 2010* Mo.2.F.1 (2010).
5. P. J. Winzer, G. Gaybon, S. Chandrasekhar, C. R. Doerr, T. Kawanishi, T. Sakamoto, and K. Higuma, in *Proceedings of OFC/NFOEC 2007* PDP24 (2007).
6. J. Ye, L. Yan, A. Yi, W. Pan, B. Luo, Z. Guo, and X. Yao, Chin. Opt. Lett. **8,** 979 (2010).
7. R. Koch, R. Noe, D. Sandel, V. Mirvoda, V. Filsinger, and K. Puntsri, in *Proceedings of OFC 2010* OThD4 (2010).
8. H. Wen, J. X. Liao, X. P. Zheng, H. Y. Zhang, and Y. L. Guo, in *Proceedings of ACP 2010* FI2 (2010).
9. Y. Shen, X. Liu, S. Zhong, J. Veselka, P. Kim, M. Frankel, and H. Sardesai, in *Proceedings of OFC 2009* JThA42 (2009).